JACS
JOURNAL OF THE AMERICAN CHEMICAL SOCIETY

pubs.acs.org/JACS

Communication

Supramolecular Nanoscaffolds within Cytomimetic Protocells as Signal Localization Hubs

Eva Magdalena Estirado,[‡] Alexander F. Mason,[‡] Miguel Ángel Alemán García, Jan C. M. van Hest,* and Luc Brunsveld*

Cite This: *J. Am. Chem. Soc.* 2020, 142, 9106–9111

Read Online

ACCESS | Metrics & More | Article Recommendations | Supporting Information

ABSTRACT: The programmed construction of functional synthetic cells requires spatial control over arrays of biomolecules within the cytomimetic environment. The mimicry of the natural hierarchical assembly of biomolecules remains challenging due to the lack of an appropriate molecular toolbox. Herein, we report the implementation of DNA-decorated supramolecular assemblies as dynamic and responsive nanoscaffolds for the localization of arrays of DNA signal cargo within hierarchically assembled complex coacervate protocells. Protocells stabilized with a semipermeable membrane allow trafficking of single-stranded DNA between neighboring protocells. DNA duplex operations demonstrate the responsiveness of the nanoscaffolds to different input DNA strands via the reversible release of DNA cargo. Moreover, a second population of coacervate protocells with nanoscaffolds featuring a higher affinity for the DNA cargo enabled chemically programmed communication between both protocell populations. This combination of supramolecular structure and function paves the way for the next generation of protocells imbued with programmable, lifelike behaviors.

The storage, manipulation, and utilization of information-rich molecules such as DNA has long been a goal in the field of bottom-up synthetic cells, alongside compartmentalization and metabolism.[1] Information processing is not only limited to DNA transcription and subsequent protein expression but also manifests as a wide range of behaviors we commonly associate with living systems, such as stimuli responsiveness, adaptability, and communication. At their core, these behaviors revolve around signal transduction, with cells sensing and responding to environmental cues. While this is a challenging concept to mimic in purely synthetic, bottom-up systems, progress is being made, and synthetic cells have been designed to transduce both chemical[2−9] and nonchemical signals such as light[10,11] or mechanical force.[12] However, many of these systems remain synthetically challenging, requiring at some point external manipulation to obtain their final structure. We present here a unique approach to obtaining signal transduction in synthetic cells, with the hierarchical organization of supramolecular components into localized signaling hubs, generating a robust, modular, and synthetically accessible protocell platform.

Complex coacervates, formed via the electrostatic complexation of oppositely charged macromolecules, are seeing increased application as bottom-up synthetic cell platforms. These crowded, highly charged, and cell-sized droplets are interesting for both their cytomimetic properties as well as their innate ability to sequester and concentrate a wide range of biologically relevant macromolecules[13−15] and functional subcompartments.[16,17] The structural stability of the otherwise rapidly coalescing coacervate droplets can successfully be controlled by the use of fatty acids,[18,19] silica nanoparticles,[17] or, in the case of the research presented herein, block copolymers.[20] This semipermeable membrane enables the sequestration of macromolecular entities and assemblies while simultaneously permitting the translocation of small molecules for signaling and catalysis.[21]

Within coacervate-based synthetic cells, the processing of information-rich molecules has predominantly been focused on the concentration and resultant enhancement in reaction kinetics of nucleotide processing enzymes[22] and the incorporation of *in vitro* transcription−translation processes.[23,24] The engineered colocalization of arrays of biomolecules inside protocells, mimicking the hierarchical self-assembly of proteins or nucleotides, has, however, seen limited attention given the lack of the appropriate molecular toolbox. In this regard, synthetic DNA-based supramolecular systems form ideal nanoscaffolds to colocalize arrays of relevant biomolecules toward the mimicry of their biological counterparts,[25−27] as its unique coded structure facilitates the design of reliable, predictable, and biocompatible interactions[28−31] such as DNA-based computing and communication in proteinosome protocells.[2] In this communication, we report utilization of a toolbox of orthogonal, hierarchical supramolecular interactions to assemble DNA localization hubs within cytomimetic particles. These unique structures are shown to transduce external chemical signals into an internal spatial organization which, when paired with the semipermeable membrane, enables interprotocell communication. This combination of

Received: February 13, 2020
Published: May 1, 2020

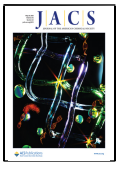

https://dx.doi.org/10.1021/jacs.0c01732
J. Am. Chem. Soc. 2020, 142, 9106–9111

supramolecular DNA nanotechnology within hierarchically organized protocells is an exciting direction and offers a range of possibilities toward the development of more elegant tools for signal localization within synthetic cells.

This system is formed via the hierarchical self-assembly of functional components (Figure 1). First, the negatively charged

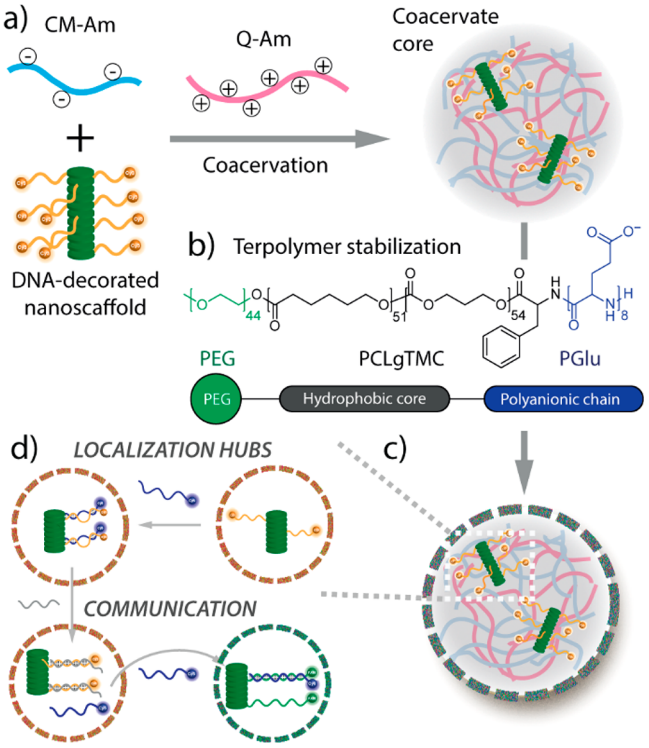

Figure 1. Depiction of protocell loading and formation. (a) Supramolecular nanoscaffold, CM-Am, and Q-Am are mixed to form coacervate microdroplets through multivalent electrostatic interactions. (b) Chemical structure of the stabilizing terpolymer, that when added to the protocells, avoids protocell coalescence and serves as a semipermeable membrane. (c) Schematic representation of the supramolecular DNA nanoscaffold inside the coacervate protocells. (d) Overview of the potential of the nanoscaffold-loaded protocell to act as a DNA localization hub and to feature programmed interprotocell communication.

supramolecular nanoscaffold and anionic carboxymethyl-functionalized amylose (CM-Am) were combined, and coacervation was initiated by the addition of amylose functionalized with a cationic quaternary amine (Q-Am). Droplet coalescence was arrested by the introduction of a synthetic block terpolymer designed with a careful balance between electrostatic, hydrophilic, and hydrophobic interactions (Figure 1b).[20] The terpolymer consists of a poly(ethylene glycol) (PEG) peripheral chain that prevents the incorporation of the terpolymer inside the coacervate droplet, a poly((ε-caprolactone)-*gradient*-(trimethylene carbonate)) (PCLgTMC) hydrophobic core to ensure the rearrangement of the terpolymer around the protocell, and a peripheral poly(glutamic acid) (PGlu) anionic chain that anchors the terpolymer to the coacervate core through long-range electrostatic interactions.[20,21]

The supramolecular nanoscaffold implemented in this study consists of previously reported amphiphilic monomers made of bis-pyridine-based C_3-symmetrical discotic molecules decorated with single-stranded DNA strands (Figure 2a). The DNA-decorated monomers self-assemble into columnar stacks, displaying multiple colocalized copies of single-stranded DNA in a quasi-1D fashion, capable of further interactions with other complementary strands via DNA duplex formation.[25,26] Nanoscaffolds were strongly sequestered within coacervate protocells with an incorporation efficiency >99%, as determined by confocal microscopy[16] (Figure 2b). The columnar stacks remained assembled upon incorporation, confirmed by bulk fluorescence spectroscopy (Figure S1) and a lack of punctae formation when only fluorescently labeled single-stranded DNA was encapsulated (Figure 2b). Control experiments revealed that sequestration of the nanoscaffold was driven by the phosphate backbone of covalently attached DNA strands, confirmed by the lackluster uptake of fluorescent dyes by themselves and DNA free, dye-labeled discotics (Figure S2). As these assemblies are approximately 100 nm long,[32] they appeared as diffraction-limited punctae. Importantly, the relatively large size of the nanoscaffolds prevent them from crossing the terpolymer membrane (Figure S3), which ensures that specific DNA sequences are unique to a protocell at formation. Furthermore, the dynamic nature of these assemblies is retained upon incorporation within the coacervate core. Time-lapse fluorescence images (Supplementary Video 1) revealed movement of the fluorescent dots, demonstrating that the nanoscaffold is not immobilized within the protocells and that the coacervate core simulates the fluidity and dynamic behavior desired for a biomimetic system. Supramolecular assembly dynamics are also retained. Increasing concentrations of DNA-functionalized monomers without Cy3-label cause a distinct increase in the emission of Cy3-labeled monomers, as fluorophores are on average further apart and thus experience lower degrees of self-quenching (Figure 2c). These results show that the assembly of this complex multicomponent system is driven by orthogonal supramolecular interactions, thus providing a robust platform within which to perform DNA-based operations.

The specific and reversible recruitment of spatially confined biomolecules in the coacervate protocell is the first step in recapitulating biomimetic signal transduction in a synthetic setting. Here, the display of high fidelity single-stranded DNA recognition sites by the supramolecular nanoscaffold opens new possibilities for the straightforward implementation of robust DNA-duplex based operations. Protocell-specific responses to external, DNA-based signals are enabled by the ability of single-stranded DNA to freely diffuse through the semipermeable membrane to find persistent, localized arrays of nanoscaffold-bound DNA. To ensure coacervate formation under the required salt conditions for hybridization (5 mM $MgCl_2$), the ratio of oppositely charged amylose derivatives was kept equivalent (1:1 mass ratio of Q-Am:CM-Am) (Figure S4). We then designed a reporting system that could rapidly indicate the assembly states of DNA signals within the coacervate protocells. This system (Figure 3) comprises a supramolecular nanoscaffold (DNA nanoscaffold **1**) that facilitates the colocalization of a complementary reporter DNA strand (Cy5-Reporter) in response to variable incoming signal DNA strands (Fuel and Antifuel). First, the Cy3-labeled DNA nanoscaffold **1** alone (at 40 nM) exhibited the characteristic fluorescent punctae when imaging with the Cy3 channel. Subsequent addition of Cy5-Reporter (5 nM) resulted in the concomitant colocalization of both dyes over 25 min, confirming DNA-duplex formation on the nanoscaffold (Figures 3a, S5). Control experiments with a mismatching

https://dx.doi.org/10.1021/jacs.0c01732
J. Am. Chem. Soc. 2020, 142, 9106−9111

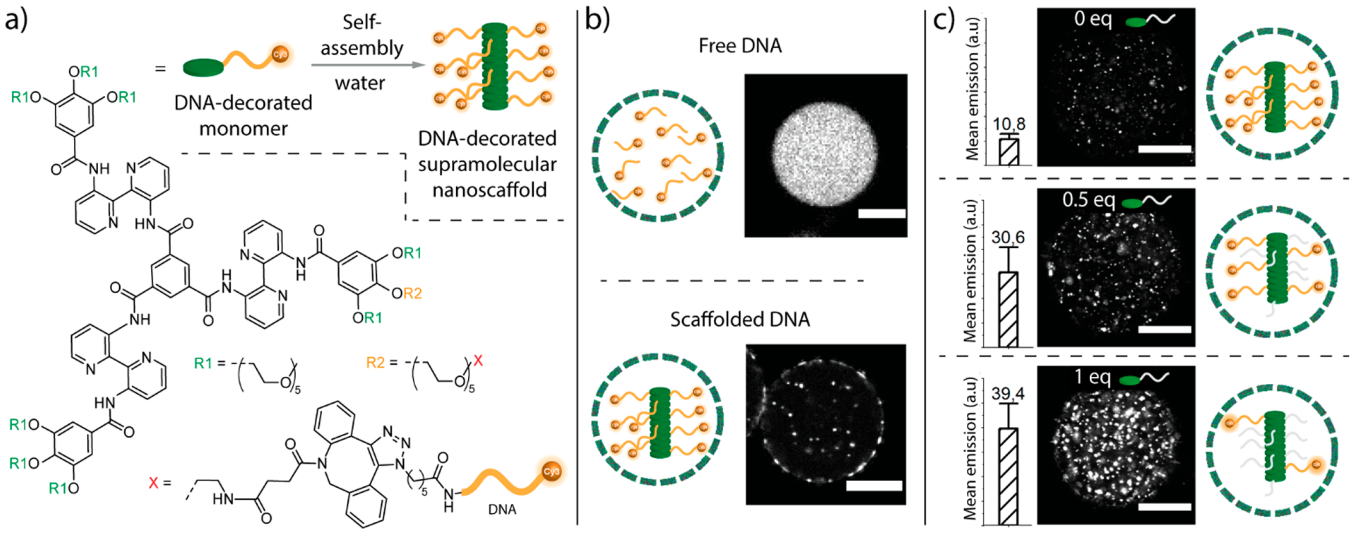

Figure 2. (a) Molecular structure of the DNA-decorated discotic monomer that self-assembles into columnar stacks in water, resulting in DNA-decorated supramolecular nanoscaffolds. (b) The negatively charged nature of DNA drives strong sequestration into coacervate protocells. Whereas ssDNA freely diffuses throughout the coacervate (top), the supramolecular nanoscaffolds force the localization of DNA templates into distinct punctae (bottom). Top and bottom scale bars represent 10 and 5 μm, respectively. (c) Dilution and subsequent dequenching of the Cy3-labeled supramolecular nanoscaffold with nonlabeled DNA-decorated monomers (white side chains) demonstrate retention of supramolecular dynamics within the coacervate. Bar graphs represent the mean Cy3 fluorescence of each coacervate. Scale bars represent 20 μm.

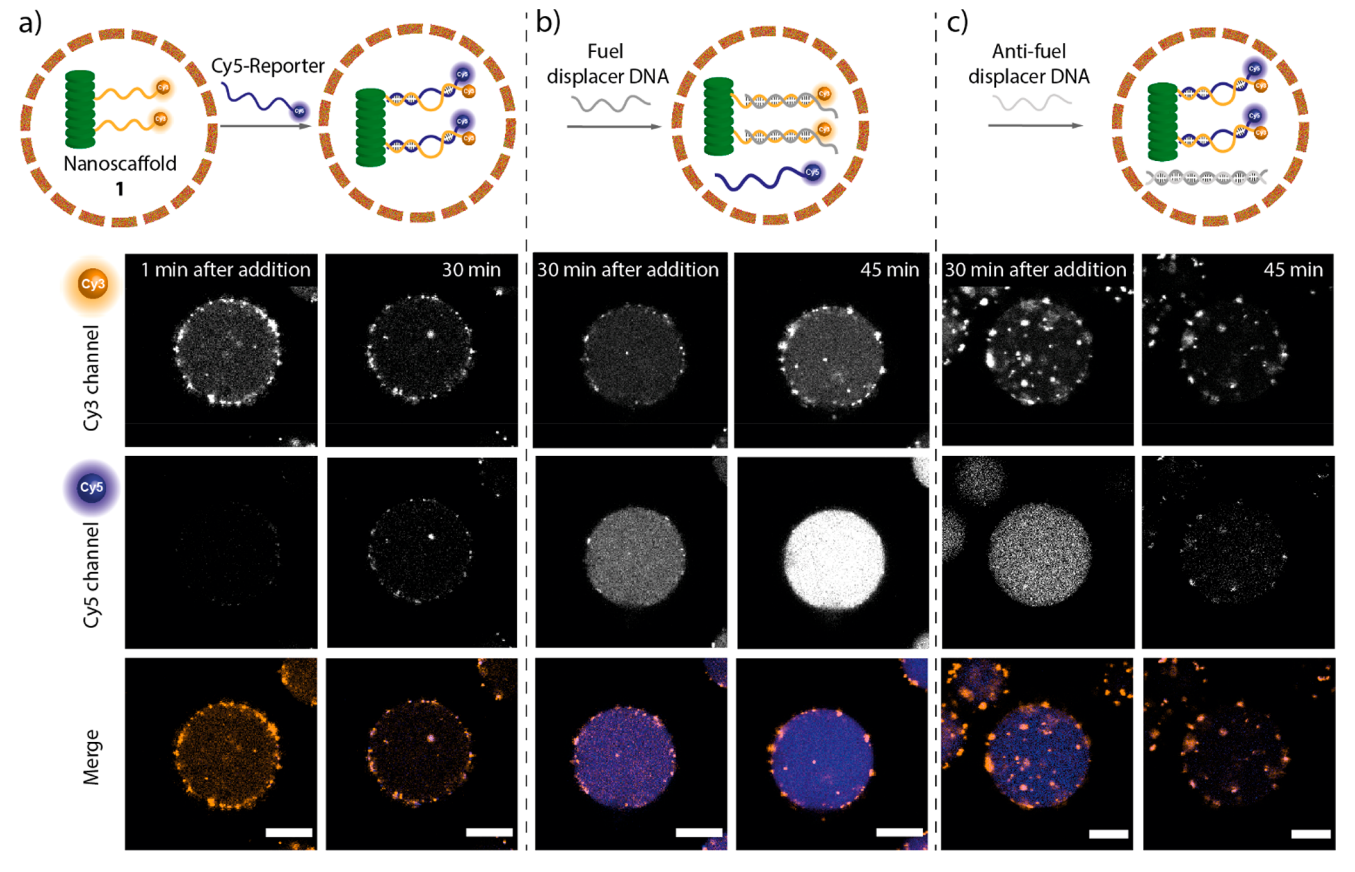

Figure 3. Schematic and accompanying single plane confocal images of nanoscaffold-mediated DNA location control. (a) Addition of complementary Cy5-Reporter strand to the exterior of protocells results in colocalization on the supramolecular nanoscaffold. (b) The spatial organization of Cy5-Reporter strand can be controlled by the addition of a Fuel displacer strand, releasing the Cy5-Reporter from the supramolecular nanoscaffold. (c) This process can be reverted by the addition of an Antifuel strand, which binds the Fuel strand and allows the Cy5-Reporter to return to the supramolecular nanoscaffold. Scale bars represent 10 μm.

supramolecular nanoscaffold together with Cy5-Reporter (Figure S6) did not feature any Cy3/Cy5 colocalization. Cy5-Reporter can be displaced from nanoscaffold **1** via so-called toehold DNA strand displacement with the addition of

https://dx.doi.org/10.1021/jacs.0c01732
J. Am. Chem. Soc. 2020, 142, 9106−9111

an external stimulus (Fuel strand, 100 nM) that features a higher affinity to nanoscaffold **1** (Figure 3b). The release of Cy5-Reporter leads to its homogeneous distribution throughout the coacervate protocell, approximately 30 min after the addition of the fuel strand. This reorganization of Cy5-Reporter within the protocell core also results in a 10-fold increase in the average intensity of the Cy5 channel (Figure S5) due to fluorescence dequenching when released from the supramolecular nanoscaffold. A concomitant increase in the Cy3 channel fluorescence intensity from the nanoscaffold is also observed. This behavior was not an artifact of heterogeneous local concentrations of reactants, as the same reorganization was observed when Cy5-Reporter was preincubated with nanoscaffold **1** for 2 h prior to Fuel strand addition to ensure complete hybridization (Figure S7).

The programmable nature of DNA allows to reverse this spatial reorganization in a sequence-specific manner. To relocalize Cy5-Reporter on nanoscaffold **1**, the Fuel strand needs to first be displaced. This was accomplished by an Antifuel strand that outcompetes nanoscaffold **1** for the Fuel strand, resulting in a clearly observable change in the distribution of Cy5-Reporter from homogeneous back to punctate, colocalized structures (Figures 3c, S5c, Supplementary Video 2). These experiments highlight the ability of this supramolecular system to receive external chemical signals and transduce them into reversible outputs, namely the protocell-wide spatial organization of macromolecules.

The ability to control the spatial organization of functional molecules coupled with a semipermeable membrane make this system an ideal candidate for cell−cell communication. This was demonstrated by the addition of a second population of coacervate protocells loaded with an analogous, FAM-labeled nanoscaffold **2** that can capture any Cy5-Reporter that is released from a separate population containing nanoscaffold **1**. The system is designed so that the diffusing Cy5-Reporter features a higher affinity for nanoscaffold **2** than for **1**. The translocation of Cy5-Reporter between neighboring coacervate populations upon the addition of Fuel strands is observable by the colocalization of Cy5/FAM in the nanoscaffold **2** population of protocells (Figures 4, S8a, Supplementary Video 3). While there is a slow background translocation of Cy5-Reporter, the addition of Fuel clearly accelerates this process (Figure S8b). Successful transmission of an information-rich signal between synthetic cells is facilitated by the semipermeable interface, which both effectively limits content mixing, creating discrete populations, while permitting free translocation of small DNA signaling strands.

Here, we demonstrated the hierarchical assembly of a synthetic cell platform capable of localized signal transduction. The electrostatically driven incorporation of supramolecular localization hubs has provided the individual protocells with information-rich signatures, enabling the binding and up-concentration of DNA-based signaling molecules at specific loci. Combined with the semipermeable terpolymer membrane, these protocells can receive and transduce external signals, effecting changes in local spatial organization and the transmission of a DNA-based reporter. This control over the positioning of information-rich molecules in bottom-up synthetic cells has important ramifications for the next generation of synthetic cells, enabling a range of biologically relevant responses to external DNA signals or for the modulation of internal structure or assembly of enzyme cascades. These responses have the potential to initiate a range of downstream processes, creating more complex, quorum-based biomimetic behaviors.

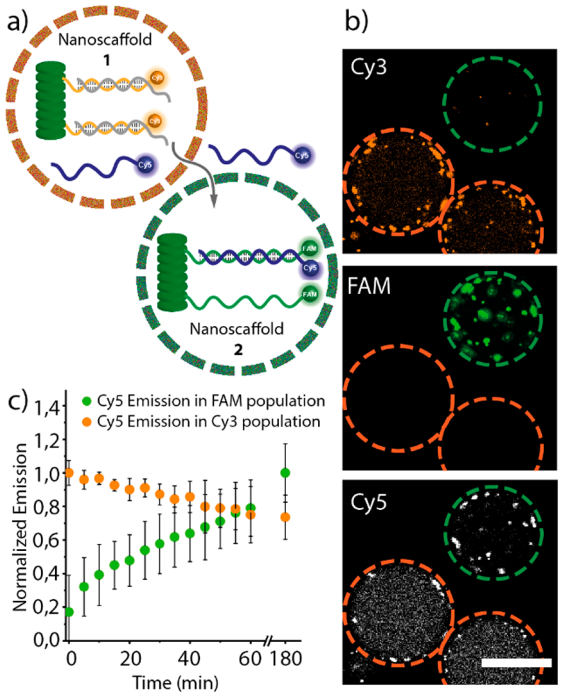

Figure 4. (a) Communication of a DNA signal between coacervate protocells loaded with supramolecular nanoscaffolds **1** and **2**. (b) Confocal microscopy images showing the Cy3, FAM, and Cy5 channels. The Cy3 channel shows the DNA colocalized arrays of nanoscaffold **1**, while the FAM channel shows the equivalent for nanoscaffold **2**. The colocalization of Cy5 dyes in the nanoscaffold **2** protocell and the reversion to a homogeneous Cy5 distribution in nanoscaffold **1** protocells after Fuel strand addition indicate successful communication between protocells. Scale bar represents 15 μm. (c) Quantification of Cy5 fluorescence within both populations over time.

■ ASSOCIATED CONTENT

Supporting Information

The Supporting Information is available free of charge at https://pubs.acs.org/doi/10.1021/jacs.0c01732.

Detailed description of materials and methods, DNA sequences, and supplementary figures (PDF)

Supplementary Video 1: Time-lapse fluorescence images of the nanoscaffolds (visible as fluorescent dots) within a protocell (AVI)

Supplementary Video 2: Spatial reorganization of Cy5-reporter strands from a dispersed localization in the protocells onto nanoscaffolds, upon liberation of the nanoscaffold from the fuel strand by addition of an antifuel strand (AVI)

Supplementary Video 3: Translocation of Cy5-reporter strands between neighboring coacervate populations featuring nanoscaffolds with different reporter affinity, upon the addition of fuel strands (MP4)

■ AUTHOR INFORMATION

Corresponding Authors

Jan C. M. van Hest − *Laboratories of Chemical Biology and Bio-Organic Chemistry, Department of Biomedical Engineering and Institute for Complex Molecular Systems, Eindhoven University of Technology, 5600MB Eindhoven, The*

https://dx.doi.org/10.1021/jacs.0c01732
J. Am. Chem. Soc. 2020, 142, 9106−9111

Netherlands; orcid.org/0000-0001-7973-2404; Email: j.c.m.v.hest@tue.nl

Luc Brunsveld − *Laboratories of Chemical Biology and Bio-Organic Chemistry, Department of Biomedical Engineering and Institute for Complex Molecular Systems, Eindhoven University of Technology, 5600MB Eindhoven, The Netherlands;* orcid.org/0000-0001-5675-511X; Email: l.brunsveld@tue.nl

Authors

Eva Magdalena Estirado − *Laboratories of Chemical Biology and Bio-Organic Chemistry, Department of Biomedical Engineering and Institute for Complex Molecular Systems, Eindhoven University of Technology, 5600MB Eindhoven, The Netherlands*

Alexander F. Mason − *Laboratories of Chemical Biology and Bio-Organic Chemistry, Department of Biomedical Engineering and Institute for Complex Molecular Systems, Eindhoven University of Technology, 5600MB Eindhoven, The Netherlands;* orcid.org/0000-0002-2847-0253

Miguel Ángel Alemán García − *Laboratories of Chemical Biology and Bio-Organic Chemistry, Department of Biomedical Engineering and Institute for Complex Molecular Systems, Eindhoven University of Technology, 5600MB Eindhoven, The Netherlands*

Complete contact information is available at: https://pubs.acs.org/10.1021/jacs.0c01732

Author Contributions

‡E.M.E. and A.F.M. contributed equally.

Funding

The Dutch Ministry of Education, Culture and Science (Gravitation program 024.001.035, VICI grant 016.150.366), the ERC Advanced grant (Artisym 694120), European Union's program Horizon 2020 Marie Curie Innovative Training Network MULTI-APP (2015−2019), and 749919-SupramolecularWires are acknowledged for funding.

Notes

The authors declare no competing financial interest.

■ ACKNOWLEDGMENTS

Dr. Jurgen Schill is thanked for providing precursor materials used in this manuscript.

■ REFERENCES

(1) Szostak, J. W.; Bartel, D. P.; Luisi, P. L. Synthesizing Life. *Nature* **2001**, *409*, 387−390.

(2) Joesaar, A.; Yang, S.; Bögels, B.; van der Linden, A.; Pieters, P.; Kumar, B. V. V. S. P.; Dalchau, N.; Phillips, A.; Mann, S.; de Greef, T. F. A. DNA-Based Communication in Populations of Synthetic Protocells. *Nat. Nanotechnol.* **2019**, *14*, 369−378.

(3) Elani, Y.; Trantidou, T.; Wylie, D.; Dekker, L.; Polizzi, K.; Law, R. V.; Ces, O. Constructing Vesicle-Based Artificial Cells with Embedded Living Cells as Organelle-like Modules. *Sci. Rep.* **2018**, *8*, 4564.

(4) Adamala, K. P.; Martin-Alarcon, D. A.; Guthrie-Honea, K. R.; Boyden, E. S. Engineering Genetic Circuit Interactions within and between Synthetic Minimal Cells. *Nat. Chem.* **2017**, *9*, 1−9.

(5) Peters, R. J. R. W.; Marguet, M.; Marais, S.; Fraaije, M. W.; van Hest, J. C. M.; Lecommandoux, S. Cascade Reactions in Multicompartmentalized Polymersomes. *Angew. Chem., Int. Ed.* **2014**, *53*, 146−150.

(6) Nijemeisland, M.; Abdelmohsen, L. K. E. A.; Huck, W. T. S.; Wilson, D. A.; van Hest, J. C. M. A Compartmentalized Out-of-Equilibrium Enzymatic Reaction Network for Sustained Autonomous Movement. *ACS Cent. Sci.* **2016**, *2*, 843−849.

(7) Lentini, R.; Martín, N. Y.; Forlin, M.; Belmonte, L.; Fontana, J.; Cornella, M.; Martini, L.; Tamburini, S.; Bentley, W. E.; Jousson, O.; Mansy, S. S. Two-Way Chemical Communication between Artificial and Natural Cells. *ACS Cent. Sci.* **2017**, *3*, 117−123.

(8) Qiao, Y.; Li, M.; Booth, R.; Mann, S. Predatory Behaviour in Synthetic Protocell Communities. *Nat. Chem.* **2017**, *9*, 110−119.

(9) Dupin, A.; Simmel, F. C. Signalling and Differentiation in Emulsion-Based Multi-Compartmentalized in Vitro Gene Circuits. *Nat. Chem.* **2019**, *11*, 32−39.

(10) Booth, M. J.; Schild, V. R.; Graham, A. D.; Olof, S. N.; Bayley, H. Light-Activated Communication in Synthetic Tissues. *Sci. Adv.* **2016**, *2*, No. e1600056.

(11) Hindley, J. W.; Elani, Y.; McGilvery, C. M.; Ali, S.; Bevan, C. L.; Law, R. V.; Ces, O. Light-Triggered Enzymatic Reactions in Nested Vesicle Reactors. *Nat. Commun.* **2018**, *9*, 3−8.

(12) Hindley, J. W.; Zheleva, D. G.; Elani, Y.; Charalambous, K.; Barter, L. M. C.; Booth, P. J.; Bevan, C. L.; Law, R. V.; Ces, O. Building a Synthetic Mechanosensitive Signaling Pathway in Compartmentalized Artificial Cells. *Proc. Natl. Acad. Sci. U. S. A.* **2019**, *116*, 16711−16716.

(13) te Brinke, E.; Groen, J.; Herrmann, A.; Heus, H. A.; Rivas, G.; Spruijt, E.; Huck, W. T. S. Dissipative Adaptation in Driven Self-Assembly Leading to Self-Dividing Fibrils. *Nat. Nanotechnol.* **2018**, *13*, 849−855.

(14) Drobot, B.; Iglesias-Artola, J. M.; Le Vay, K.; Mayr, V.; Kar, M.; Kreysing, M.; Mutschler, H.; Tang, T. D. Compartmentalised RNA Catalysis in Membrane-Free Coacervate Protocells. *Nat. Commun.* **2018**, *9*, 3643.

(15) Martin, N.; Tian, L.; Spencer, D.; Coutable-Pennarun, A.; Anderson, J. L. R.; Mann, S. Photoswitchable Phase Separation and Oligonucleotide Trafficking in DNA Coacervate Microdroplets. *Angew. Chem., Int. Ed.* **2019**, *58*, 14594−14598.

(16) Mason, A. F.; Yewdall, N. A.; Welzen, P. L. W.; Shao, J.; van Stevendaal, M.; van Hest, J. C. M.; Williams, D. S.; Abdelmohsen, L. K. E. A. Mimicking Cellular Compartmentalization in a Hierarchical Protocell through Spontaneous Spatial Organization. *ACS Cent. Sci.* **2019**, *5*, 1360−1365.

(17) Kumar, P. B. V. V. S.; Fothergill, J.; Bretherton, J.; Tian, L.; Patil, A. J.; Davis, S. A.; Mann, S. Chloroplast-Containing Coacervate Micro-Droplets as a Step towards Photosynthetically Active Membrane-Free Protocells. *Chem. Commun.* **2018**, *54*, 3594−3597.

(18) Tang, T.-Y. D.; Hak, C. R. C.; Thompson, A. J.; Kuimova, M. K.; Williams, D. S.; Perriman, A. W.; Mann, S.; Tang, T.-Y. D.; Hak, C.; Thompson, A. J.; Kuimova, M. K.; Williams, D. S.; Perriman, A. W.; Mann, S. Fatty Acid Membrane Assembly on Coacervate Microdroplets as a Step towards a Hybrid Protocell Model. *Nat. Chem.* **2014**, *6*, 527−533.

(19) Pir Cakmak, F.; Grigas, A. T.; Keating, C. D. Lipid Vesicle-Coated Complex Coacervates. *Langmuir* **2019**, *35*, 7830−7840.

(20) Mason, A. F.; Buddingh', B. C.; Williams, D. S.; van Hest, J. C. M. Hierarchical Self-Assembly of a Copolymer-Stabilized Coacervate Protocell. *J. Am. Chem. Soc.* **2017**, *139*, 17309−17312.

(21) Yewdall, N. A.; Buddingh, B. C.; Altenburg, W. J.; Timmermans, S. B. P. E.; Vervoort, D. F. M.; Abdelmohsen, L. K. E. A.; Mason, A. F.; Hest, J. C. M. Physicochemical Characterization of Polymer-Stabilized Coacervate Protocells. *ChemBioChem* **2019**, *20*, 2643−2652.

(22) Bevilacqua, P. C.; Poudyal, R. R.; Guth-Metzler, R. M.; Veenis, A. J.; Keating, C. D.; Frankel, E. A. Template-Directed RNA Polymerization and Enhanced Ribozyme Catalysis inside Membraneless Compartments Formed by Coacervates. *Nat. Commun.* **2019**, *10*, 1−13.

(23) Tang, T.-Y. D.; van Swaay, D.; DeMello, A.; Ross Anderson, J. L.; Mann, S. Vitro Gene Expression within Membrane-Free Coacervate Protocells. *Chem. Commun.* **2015**, *51*, 11429−11432.

(24) Sokolova, E.; Spruijt, E.; Hansen, M. M. K.; Dubuc, E.; Groen, J.; Chokkalingam, V.; Piruska, A.; Heus, H. A.; Huck, W. T. S.

Enhanced Transcription Rates in Membrane-Free Protocells Formed by Coacervation of Cell Lysate. *Proc. Natl. Acad. Sci. U. S. A.* **2013**, *110*, 11692−11697.
(25) Alemán García, M. Á.; Magdalena Estirado, E.; Milroy, L.-G.; Brunsveld, L. Dual-Input Regulation and Positional Control in Hybrid Oligonucleotide/Discotic Supramolecular Wires. *Angew. Chem., Int. Ed.* **2018**, *57*, 4976−4980.
(26) Magdalena Estirado, E.; Aleman Garcia, M. A.; Schill, J.; Brunsveld, L. Multivalent Ultrasensitive Interfacing of Supramolecular 1D Nanoplatforms. *J. Am. Chem. Soc.* **2019**, *141*, 18030−18037.
(27) Wijnands, S. P. W.; Engelen, W.; Lafleur, R. P. M.; Meijer, E. W.; Merkx, M. Controlling Protein Activity by Dynamic Recruitment on a Supramolecular Polymer Platform. *Nat. Commun.* **2018**, *9*, 65.
(28) Vybornyi, M.; Vyborna, Y.; Häner, R. DNA-Inspired Oligomers: From Oligophosphates to Functional Materials. *Chem. Soc. Rev.* **2019**, *48*, 4347−4360.
(29) Engelen, W.; Zhu, K.; Subedi, N.; Idili, A.; Ricci, F.; Tel, J.; Merkx, M. Programmable Bivalent Peptide−DNA Locks for PH-Based Control of Antibody Activity. *ACS Cent. Sci.* **2020**, *6*, 22−31.
(30) Lacroix, A.; Vengut-Climent, E.; de Rochambeau, D.; Sleiman, H. F. Uptake and Fate of Fluorescently Labeled DNA Nanostructures in Cellular Environments: A Cautionary Tale. *ACS Cent. Sci.* **2019**, *5*, 882−891.
(31) Platnich, C. M.; Hariri, A. A.; Sleiman, H. F.; Cosa, G. Advancing Wireframe DNA Nanostructures Using Single-Molecule Fluorescence Microscopy Techniques. *Acc. Chem. Res.* **2019**, *52*, 3199−3210.
(32) van Dun, S.; Schill, J.; Milroy, L.-G.; Brunsveld, L. Mutually Exclusive Cellular Uptake of Combinatorial Supramolecular Copolymers. *Chem. - Eur. J.* **2018**, *24*, 16445−16451.

https://dx.doi.org/10.1021/jacs.0c01732
J. Am. Chem. Soc. 2020, 142, 9106−9111